Pis'ma v ZhETF, vol. 85, iss. 7, pp. 387 – 392

Color dipoles, PCAC and Adler's theorem

R. Fiore[1)*], *V. R. Zoller*[1)+]

*Dipartimento di Fisica, Università della Calabria

*Istituto Nazionale di Fisica Nucleare, Gruppo collegato di Cosenza, I-87036 Rende, Cosenza, Italy

+Institute for Theoretical and Experimental Physics, 117218 Moscow, Russia

Submitted 28 February 2007

Being reformulated in the color dipole basis of small-x QCD Adler's theorem establishes a connection between perturbative and non-perturbative descriptions of DIS and quantifies the effect of non-perturbative dynamics on would-be-perturbative observables. In particular, it provides a quantitative measure of the non-perturbative influence on the longitudinal structure function in charged current DIS and imposes stringent constraints on non-perturbative parameters of color dipole models. Our analysis calls for new experimental tests of Adler's theorem in diffractive neutrino scattering.

PACS: 12.38.–t

1. Introduction. Adler's theorem [1] connects charged current DIS (deep inelastic scattering) with soft hadronic physics. Here we study its efficiency as a constraint on parameters of color dipole models intended to describe phenomenologically both soft and hard dynamics of DIS processes. We focus on the vacuum exchange dominated leading $\log(1/x)$ region of large Regge parameter $x^{-1} \gtrsim 10^2$ which is

$$x^{-1} = 2m_N\nu/(m_A^2 + Q^2). \qquad (1)$$

In (1) ν and Q^2 are the laboratory frame energy and virtuality of the probe, respectively. The parameter $m_A \simeq 1$ GeV serves to define the mass scale in the light-flavor axial channel. We base our consideration on the color dipole (CD) approach to the BFKL [2], evolution of small-x DIS [3, 4]. In this approach the interaction of high-energy neutrino with the target nucleon, viewed in the laboratory frame, derives from the coherent interaction of $q\bar{q}, q\bar{q}g, \dots$ states in the light-cone electro-weak (EW) boson. At small x the color dipole size, $\mathbf{r}$, of the constituent quark-antiquark pair is conserved in the interaction process and the absorption cross section for the EW boson in the helicity state λ is calculated as the quantum mechanical expectation value of the flavor independent CD cross section $\sigma(x,r)$,

$$\sigma_\lambda(x,Q^2) = \langle \Psi_\lambda(z,\mathbf{r})|\sigma(x,r)|\Psi_\lambda(z,\mathbf{r})\rangle. \qquad (2)$$

The CD structure of the W-boson is described by the light-cone wave function (LCWF) of the quark-antiquark state $\Psi_\lambda(z,\mathbf{r})$ [5, 6]. An interesting possibility to gain deeper insight into the dynamics of small and large color dipoles is offered by the neutrino DIS in the axial channel. In the axial channel at $Q^2 \to 0$ the light-cone wave function of the longitudinal W boson is proportional of the divergence of the axial-vector current, $\Psi_L \propto \partial_\mu A_\mu$. The PCAC (partially conserved axial-vector current) relation [7], $\partial_\mu A_\mu = m_\pi^2 f_\pi \varphi$, connects via Adler's theorem [1] the longitudinal cross section σ_L defined by Eq.(2) and the on-shell pion-nucleon total cross section $\sigma_\pi = \langle \Psi_\pi(z,\mathbf{r})|\sigma(x,r)|\Psi_\pi(z,\mathbf{r})\rangle$,

$$\lim_{Q^2\to 0} Q^2\sigma_L(x,Q^2) = g^2 f_\pi^2 \sigma_\pi(\nu). \qquad (3)$$

In Eq.(3) ν and x are linked by the Eq.(1). The weak charge g in (3) is related to the Fermi coupling constant G_F,

$$G_F/\sqrt{2} = g^2/m_W^2, \qquad (4)$$

and $f_\pi \simeq 131$ MeV is the pion decay constant. The Eq.(3) connects absorption cross sections of two high-energy projectiles having very different CD structure, the pointlike W and the non-pointlike π. While the light-cone wave function of the pion $\Psi_\pi(z,\mathbf{r})$ is smooth and finite at small [2)] r, the EW boson wave function is singular, $\Psi_L \sim r^{-1}$. This singularity is a legitimate pQCD effect and it makes evaluation of hard contributions to $Q^2\sigma_L(x,Q^2)|_{Q^2\to 0}$ more reliable. In particular, this singularity uniquely predicts that the small dipole (hard) contribution to σ_L is much stronger than to σ_π.

Since the pioneering paper [10], where the axial-vector meson dominance (AVMD) was suggested,

---

[1)] e-mail: fiore@cs.infn.it, zoller@itep.ru

[2)] For a review of the dominance of the soft LCWF and references see [8, 9].

Adler's theorem has been considered as a relation between the higher mass contributions to the axial current and the pion-nucleon cross section. The AVMD was successfully applied to the analysis of the coupled-channel problem of neutrino-nucleus interactions in Refs. [11 – 13] where the mechanism of the $\rho\pi$ dominance was analyzed in detail. In Ref. [14] the PCAC component of the cross section was identified with the longitudinal part of the a_1-meson and the constraint for the longitudinal AVMD DIS structure function was obtained. Thus, in the AVMD representation Adler's theorem relates so to say soft physics to soft physics, the pion to higher axial-vector excitations. Only in the CD basis Adler's theorem gains its rightful heuristic power. It establishes a connection between perturbative and non-perturbative processes and shows the effect, if not reveals a mechanism, of non-perturbative dynamics on would-be-perturbative observables. In particular, it provides a quantitative measure of the non-perturbative influence on the longitudinal structure function of the light-flavor charged current (CC) DIS. Below we discuss the origin and consequences of this observation.

2. Adler's theorem and the axial mass scale. The CD approach [15, 16] proved to be very successful in describing of inclusive and diffractive electroproduction DIS data in the vector channel down to $Q^2 \sim m_q^2$, where m_q is the constituent quark mass (for the review see [17] and also [18]). The mass scale in the vector channel is fixed by the mass of lightest vector mesons, $m_V \sim 1\,\text{GeV}$. In the axial channel the spectrum of hadronic excitations starts with the nearly massless pion. To get an idea of the characteristic axial mass scale let us turn to Adler's theorem. Following Adler [1], consider the particular case of forward lepton production in the reaction of neutrino-nucleon scattering

$$\nu(k) + N(p) \to l(k') + X(p_X) \tag{5}$$

in the limit $Q^2 = -q^2 \to 0$ and suppose that ${k'}^2 = m_l^2 = 0$. In (5) p_X is the 4-momentum of the final hadronic state X, k and k' are the 4-momenta of the neutrino and final lepton and $q = k - k'$ is the 4-momentum carried by W-boson. The amplitude of the process (5) is

$$M = \frac{G_F}{\sqrt{2}} l_\mu \langle X|J_\mu|p\rangle. \tag{6}$$

The massless leptonic current l_μ is conserved and at $Q^2 \to 0$ is proportional to q_μ,

$$l_\mu = \bar{u}_l(k')\gamma_\mu(1-\gamma_5)u_\nu(k) = \frac{4\sqrt{1-y}}{y} q_\mu, \tag{7}$$

where $y = pq/kp = \nu/E$. The divergence of the vector component of the hadronic current $J_\mu = V_\mu - A_\mu$ is supposed to be zero. Let $\langle X|A_\mu|p\rangle = M_\mu$ be the sum of the pion pole term and amplitudes of higher axial-vector hadronic states, $|a\rangle$,

$$M_\mu = M_\mu^\pi + \sum_{a\neq\pi} M_\mu^a. \tag{8}$$

In (8)

$$M_\mu^\pi = i q_\mu f_\pi \frac{1}{Q^2 + m_\pi^2} M_\pi. \tag{9}$$

Since $q_\mu l_\mu = 0$, the pion pole does not contribute to $l_\mu M_\mu$ and M is saturated by higher axial-vector states [19]

$$M = \frac{G_F}{\sqrt{2}} \sum_{a\neq\pi} l_\mu M_\mu^a. \tag{10}$$

So, the mass scale in the axial channel has been determined, in fact, in experiments on the diffraction dissociation of high-energy pions, where the mass spectrum of final $a_1, \rho\pi, \pi\pi\pi$... states was measured (see [20] and also the discussion in [11]).

Adler's amplitude is linear in the divergence of the axial current. To this accuracy, making use of $q_\mu M_\mu = 0$ and

$$\sum_{a\neq\pi} q_\mu M_\mu^a = i f_\pi M_\pi \tag{11}$$

– the Goldberger-Treiman conspiracy [21], – yields the neutrino amplitude which is multiple of the pion amplitude

$$M = \frac{i G_F f_\pi}{\sqrt{2}} \frac{4\sqrt{1-y}}{y} M_\pi. \tag{12}$$

Summing over all final hadronic states one arrives at Adler's relation between $\sigma_\pi(\nu)$ and the double differential cross section of the process (5),

$$\left.\frac{d\sigma}{dydQ^2}\right|_{Q^2=0} = \frac{\pi}{(pk)}\frac{1}{(4\pi)^3}\sum_X |M|^2 (2\pi)^4 \delta^{(4)}(p+q-p_X) = \frac{G_F^2}{2\pi^2}\frac{1-y}{y} f_\pi^2 \sigma_\pi(\nu). \tag{13}$$

3. CD models and the axial mass scale again. CD models rely upon the small-x flux-cross section factorization,

$$yQ^2 \frac{d\sigma}{dydQ^2} = f_\lambda \sigma_\lambda. \tag{14}$$

The fluxes f_λ and cross sections σ_λ depend on the polarization state λ of the EW boson. In the W-proton collision frame $q_\mu = (\nu, 0, 0, q_z)$. and the 4-vector of the so called longitudinal polarization, which we are interested in, is

$$s_\mu = \frac{1}{\sqrt{Q^2}}(q_z, 0, 0, \nu) = \frac{\sqrt{Q^2}}{\sqrt{(pq)^2 + m_N^2 Q^2}} \left(p_\mu + \frac{pq}{Q^2} q_\mu \right). \tag{15}$$

Throughout this paper we use, following tradition, the name "longitudinal" for the time-like vector s_μ and provide corresponding variables with the label L. Then, in close similarity with the QED flux of longitudinal photons, the flux of W_L-bosons is

$$f_L = \frac{4\alpha_W}{\pi} \frac{Q^4}{m_W^4}(1 - y), \tag{16}$$

where $\alpha_W = g^2/4\pi$. Applying the optical theorem to the amplitude for Compton scattering of the W_L yields

$$\frac{d\sigma}{dydQ^2}\Big|_{Q^2=0} = \frac{G_F^2}{2\pi^2} \frac{(1-y)}{y} \frac{Q^2}{g^2} \sigma_L(x, Q^2)\Big|_{Q^2=0}, \tag{17}$$

where, in the fixed-$\mathbf{r}$ representation,

$$\begin{aligned} \sigma_L(x, Q^2) &= \langle W|\mathbf{r}\rangle\langle\mathbf{r}|\hat\sigma|\mathbf{r}\rangle\langle\mathbf{r}|W\rangle = \\ &= \int dz d^2\mathbf{r} |\Psi_L(z, \mathbf{r})|^2 \sigma(x, r). \end{aligned} \tag{18}$$

The Eq.(3) then follows from comparison of Eqs. (13) and (17). In Eq. (18) $\langle\mathbf{r}|\hat\sigma|\mathbf{r}\rangle = \sigma(x, r)$, $\hat\sigma$ is the cross section operator and $\langle\mathbf{r}|W\rangle = \Psi_L(z, \mathbf{r})$ is the LCWF of the $|u\bar d\rangle$ state with the u quark carrying fraction z of the W^+ light-cone momentum and $\bar d$ with momentum fraction $1 - z$ (see [5] for details). In [5] we used for Ψ_L the notation Ψ_0. The expansion (8) is written in the basis of physical hadrons (mass operator eigenstates) $|a\rangle$ related to fixed-$\mathbf{r}$ states via $|\mathbf{r}\rangle = \sum_a \langle a|\mathbf{r}\rangle|a\rangle$. In this basis the diagonal matrix elements of $\hat\sigma$ give the total cross section of $a - N$ scattering, $\sigma_a = \langle a|\hat\sigma|a\rangle$ [22], and Eq.(18) turns into

$$\begin{aligned} Q^2\sigma_L\Big|_{Q^2=0} &= Q^2\langle W|\mathbf{r}\rangle\langle\mathbf{r}|\hat\sigma|\mathbf{r}\rangle\langle\mathbf{r}|W\rangle = \\ &= Q^2 \sum_{a,a'\neq\pi} \langle W|a\rangle\langle a|\hat\sigma|a'\rangle\langle a'|W\rangle = \\ &= Q^2\langle W|\pi\rangle\langle\pi|\hat\sigma|\pi\rangle\langle\pi|W\rangle = g^2 f_\pi^2 \sigma_\pi. \end{aligned} \tag{19}$$

In (19) the Goldberger-Treiman conspiracy, Eq.(11), was used to come from the second line to the third one.

Notice that the sum over hadronic states $|a\rangle$ in (19) does not include the pion, the W-boson in the polarization state s_μ (see Eq.(15)) does not mix with the pion, $s_\mu q_\mu = 0$. Consequently, the CD states described by the light-cone wave function $\Psi_L(z, \mathbf{r})$ in Eq.(18) are dual not to the nearly massless π-meson but to "normal" axial-vector hadronic states $(a_1, \rho\pi, \ldots)$ of a mass $\sim 1\,\mathrm{GeV}$. This observation justifies, in particular, the choice of the mass scale $m_A = 1\,\mathrm{GeV}$ in Eq.(1) and lends support to the CD description of small-x phenomena in the axial channel.

4. F_L-f_π-σ_π-correlation in color dipole basis. In terms of the longitudinal structure function

$$F_L(x, Q^2) = \frac{Q^2}{4\pi^2\alpha_W}\sigma_L(x, Q^2), \tag{20}$$

Eq.(19) can be rewritten as

$$F_L(x, 0) = \frac{f_\pi^2}{\pi}\sigma_\pi(\nu), \tag{21}$$

where ν is related to x by Eq.(1). In (20) $\sigma_L(x, Q^2)$ is defined by the CD factorization equation (18) and the light-cone density of CD states $u\bar d, c\bar s, \ldots$ is

$$|\Psi_L(z, \mathbf{r})|^2 = |V_L(z, \mathbf{r})|^2 + |A_L(z, \mathbf{r})|^2,$$

with

$$\begin{aligned} |V_L(z, \mathbf{r})|^2 &= \frac{2\alpha_W N_c}{(2\pi)^2 Q^2} \big\{ \big[2Q^2 z(1-z) + \\ &+ (m-\mu)[(1-z)m - z\mu]\big]^2 K_0^2(\varepsilon r) + \\ &+ (m-\mu)^2\varepsilon^2 K_1^2(\varepsilon r)\big\}, \end{aligned} \tag{22}$$

$$\begin{aligned} |A_L(z, \mathbf{r})|^2 &= \frac{2\alpha_W N_c}{(2\pi)^2 Q^2} \big\{ \big[2Q^2 z(1-z) + \\ &+ (m+\mu)[(1-z)m + z\mu]\big]^2 K_0^2(\varepsilon r) + \\ &+ (m+\mu)^2\varepsilon^2 K_1^2(\varepsilon r)\big\}, \end{aligned} \tag{23}$$

where m and μ are the quark and antiquark masses and $\varepsilon^2 = z(1-z)Q^2 + (1-z)m^2 + z\mu^2$ [5, 6]. At $Q^2 \to 0$ and for equal masses of constituent quarks $m = \mu = m_q$, the axial-vector light-cone density of $u\bar d$ states does not depend on z and is as follows

$$|\Psi_L(r)|^2 = \frac{2\alpha_W N_c}{\pi^2} \frac{m_q^2}{Q^2} \left[m_q^2 K_0^2(m_q r) + m_q^2 K_1^2(m_q r) \right]. \tag{24}$$

At $y \lesssim 1$, $K_0(y) \sim \log(1/y)$ and $K_1(y) \sim 1/y$. Then, from Eqs. (20) and (24)

$$F_L(x, 0) \sim \frac{N_c m_q^2}{2\pi^3} \int_0^{m_q^{-2}} \frac{dr^2}{r^2} \sigma(x, r). \tag{25}$$

The CD cross section is $\sigma(x, r) = r^2 C(x, r)$ with $C(x, r)$ slowly varying with r. For small dipoles $C(x, r)$ depends on r only logarithmically. For large dipoles, such that $r > r_s$, $\sigma(x,r)$ saturates and $C(x,r) = \sigma_s(x)/r^2$ [15]. Therefore F_L depends on several non-perturbative parameters, m_q, r_s and [3] σ_s, and, because of the axial current non-conservation, it is sensitive to the value of the constituent quark mass,

$$F_L \propto m_q^2 \sigma_s \log[1 + 1/(m_q r_s)^2]. \qquad (26)$$

The sensitivity is lost, however, for $m_q^2 \gg r_s^{-2}$.

The *rhs* of Eq.(21) is known experimentally with high accuracy and, in view of all theoretical uncertainties with non-perturbative effects, Eq.(21) could be considered as a very useful constraint on parameters of CD models. Let us start, however, with a self-consistency check and before imposing experimental bounds on f_π and σ_π let us evaluate F_L, f_π and σ_π within the LCWF CD technique. Then, the deviation of the ratio

$$R_{PCAC} = \frac{\pi F_L(x,0)}{f_\pi^2 \sigma_\pi(\nu)}. \qquad (27)$$

from unity may serve as the measure of accuracy of the approach. Because of (26) the dependence of f_π and σ_π on the constituent quark mass is of prime importance here.

Notice first, that contrary to the pointlike probe, the dipole size of the non-pointlike pion and, consequently, the value of σ_π is determined not by m_q but by an additional parameter R which introduces the intrinsic momentum cut-off [4]. The latter removes the small-r singularity from $\Psi_\pi(z,r)$ and, simultaneously, ensures the correct value of the charge radius of the pion. The dependence of σ_π on m_q appears to be marginal and

$$\sigma_\pi = \langle \Psi_\pi(z,\mathbf{r}) | \sigma(x,r) | \Psi_\pi(z,\mathbf{r}) \rangle \sim r_\pi^2 C(x, r_\pi). \qquad (28)$$

The quantity which is very sensitive to m_q is the pion decay constant [23, 24],

$$f_\pi = \frac{m_q N_c}{4\pi^3} \int \frac{dz d^2\mathbf{k}}{z(1-z)} \Psi_\pi(M^2). \qquad (29)$$

To a crude approximation, $f_\pi \propto m_q$ and for $m_q R \ll 1$ (in [23] $R = 2.2\,\mathrm{GeV}^{-1}$)

$$f_\pi \propto m_q \sqrt{\log(2/m_q R)}.$$

[3] There is, of course, one more (hidden) non-perturbative parameter – the axial charge g_A. The renormalization of g_A is neglected here and the ratio g_A/g_V for constituent quarks is assumed to be the same as for current quarks, $g_A/g_V = 1$.

[4] The radial part of Ψ_π in momentum space is $\Psi_\pi(M^2) \propto M^{-2}\exp[-\frac{1}{8}R^2M^2]$ [23] (see also [24]), where M stands for the invariant mass of the light-cone $q\bar{q}$ state and $M^2 = (m_q^2 + \mathbf{k}^2)/z(1-z)$.

This gives a chance to satisfy (21) adjusting properly non-perturbative parameters.

Invoking the CD factorization, which is valid for soft as well as for hard diffractive interactions, we evaluate the vacuum exchange contribution to $F_L(x,0)$ and $\sigma_\pi(\nu)$. The structure function $F_L(x,0)$ comes from Eqs.(18), (20), (24) with $m_q = 150\,\mathrm{MeV}$, the value commonly used now in CD models successfully tested against DIS data. The $\log(1/x)$-evolution of $\sigma(x,r)$ is described by the CD BFKL equation [25, 26]. Corresponding boundary condition is found in [27]. With the pion LCWF of Ref.[23] we obtain σ_π shown in Fig.1 (right panel) by the dashed line. The ν-dependence of

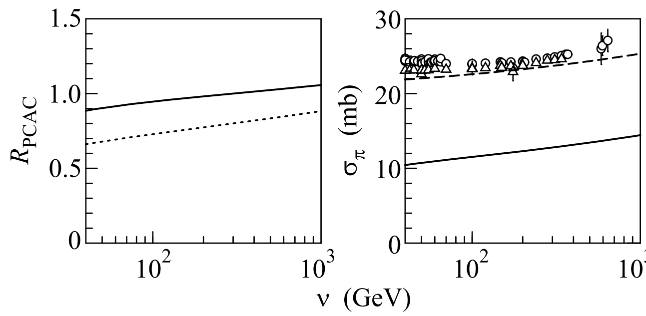

Fig.1. Left panel: the ratio R_{PCAC} as a function of ν evaluated with the pion LCWF of Ref.[23] for $m_q = 150$ MeV – solid line; the ratio R_{PCAC} with the pion LCWF of Ref.[24] and $m_q = 250\,\mathrm{MeV}$ – dotted line. Right panel: the CD BFKL evaluation of $\sigma_\pi(\nu)$ – dashed line. Data points (triangles and circles) are measurements of total $\pi^+ p$ and $\pi^- p$ cross sections, respectively [28]. Also shown by the solid line is the quantity $\sigma_{PCAC}(\nu)$ for the empirical value of f_π and with F_L evaluated for $m_q = 150\,\mathrm{MeV}$

R_{PCAC} is shown in Fig.1 (left panel) by the solid line. With certain reservations about the slope of $R_{PCAC}(\nu)$ (see below) we conclude that our CD model successfully passed the consistency test. However, this “purely theoretical” approach to Adler's theorem is not quite satisfactory. The point is that the constituent quark with $m_q = 150\,\mathrm{MeV}$ amounts to $f_\pi = 96\,\mathrm{MeV}$ *vs.* the empirical value $f_\pi = 130.7 \pm 0.46\,\mathrm{MeV}$ [28]: not quite bad for the model evaluation of the soft parameter f_π, although not satisfactory either. Within the model [23] $f_\pi = 131\,\mathrm{MeV}$ corresponds to $m_q = 245\,\mathrm{MeV}$, the value which is very close to $m_q = 250\,\mathrm{MeV}$ of Ref.[24]. In [24] an oscillator type ansatz for the pion LCWF was used and good agreement of predictions of the model with both the empirical value of the pion decay constant and the charge radius of the pion was found. The ratio R_{PCAC} evaluated with the pion LCWF of Ref.[24] is shown in Fig.1 (left panel) by the dotted line. Evidently, making the light quark heavier affects the distribution of color dipoles in the light-cone W_L-boson in such a way that the characteristic dipole sizes contributing to F_L, $r^2 \lesssim m_q^{-2}$ (mind also the small-r singularity in Ψ_L), becomes much smaller than those contributing to σ_π, $r^2 \sim r_\pi^2 \simeq 1.2\,\mathrm{fm}^2$. The BFKL $\log(1/x)$-evolution of dipole cross sections is characterized by the exponent $\Delta(x, r)$ of the local x-dependence of

$$\sigma(x, r) \propto \exp[-\Delta(x, r) \log(1/x)]; \qquad (30)$$

$\Delta(x, r)$ varies with r and $\Delta(x, r_1) > \Delta(x, r_2)$ for $r_1 < r_2$ [25]. Hence, the structure function $F_L(x, 0)$ growing with ν faster than $\sigma_\pi(\nu)$ in conflict with the requirement of Eq.(21).

As we noted above Eq.(21) can be considered as a condition on parameters of CD models. To see its restrictive power in action one can construct the quantity

$$\sigma_{PCAC}(\nu) = \pi F_L(x, 0)/f_\pi^2, \qquad (31)$$

with the empirical value of $f_\pi = 130.7\,\mathrm{MeV}$ and compare its ν-dependence with experimental data on $\sigma_\pi(\nu)$. Our $\sigma_{PCAC}(\nu)$ is shown by the solid line in Fig.1 (right panel). It strongly undershoots $\sigma_\pi(\nu)$ thus indicating that $F_L(x, 0)$ evaluated with $m_q = 150\,\mathrm{MeV}$ fails to satisfy the Eq.(21). We tried also the CD cross sections of Refs.[18]. Corresponding F_L proved to be close to ours. Notice that, the discrepancy observed may have the same origin as the deficit of the differential cross section of diffractive vector meson production found in [29]. That calls for better understanding of the infrared properties of the CD cross section.

From a different point of view, good agreement with data of both $\sigma_\pi(\nu)$ and f_π spoiled, however, by the under-predicted $F_L(x.0)$ implies that non-perturbative interactions in the axial channel blow-up the dipole size and, in the spirit of PCAC, $\sqrt{Q^2}\Psi_L(z, \mathbf{r}) \to g f_\pi \Psi_\pi(z, \mathbf{r})$ at $Q^2 \to 0$.

5. Weak current non-conservation and charm-strange dominance. One more concluding remark is on the role of charm-strange current. The structure function $F_L(x, 0)$ shown in Fig.1 does not contain the cs-current contribution. The latter is presented in Fig.2 were the ud-term and the sum $ud + cs$ are shown separately for different virtualities of the probe. For the cs-current $x = x_{Bj}(1 + M_{cs}^2/Q^2)$ with $M_{cs}^2 = 4$ GeV^2. Eqs.(22), (23) make it clear that it is the non-conservation of both axial-vector and vector currents what leads to the charm-strange dominance in $F_L(x, Q^2)$ at small x.

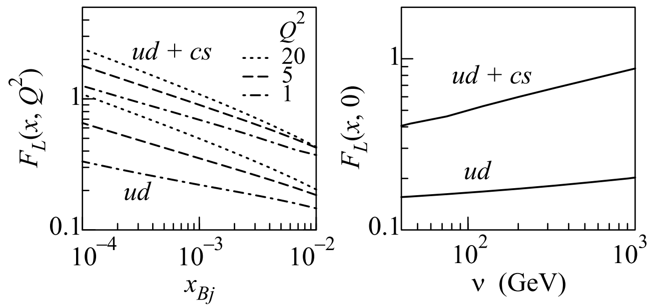

Fig.2. Left panel: three lower lines represent the ud-current contribution to $F_L(x, Q^2)$ as a function of Bjorken variable denoted by x_{Bj} for different values of Q^2 given in GeV^2. Three upper lines correspond to the sum of ud- and cs-current contributions to F_L. Right panel: F_L as a function of ν for $Q^2 = 0$

6. Summary and conclusions. Summarizing, we considered the PCAC hypothesis in a specific domain of small Bjorken x, where the relevant degrees of freedom are the QCD color dipoles. We reformulated Adler's theorem in the CD basis and analyzed its efficiency as a constraint requiring identical cross sections for scattering processes with pointlike and non-pointlike probes. This requirement, with certain reservations about absorption/unitarity corrections, was found hard to meet within the color dipole models successfully tested against HERA data. Corresponding non-perturbative parameters including m_q were adjusted to pave the way from the region $Q^2 \simeq m_q^2$ to high-Q^2 DIS. The analysis of diffractive vector mesons [29] shows that the adjustment is not perfect. The discrepancy found in our paper can be understood as the non-perturbative effect of increasing dipole size of the light-cone W_L-boson at $Q^2 \to 0$. Adler's theorem provides its quantitative measure. This observation makes topical new experimental tests of Adler's theorem in the diffraction region of $x \lesssim 0.01$. In view of the charm-strange dominance discussed above (which also should be tested experimentally) the cs-current contribution to the differential cross section $d\sigma/dydQ^2$ of the reaction (5) has to be isolated properly to separate the PCAC term.

Thanks are due to N.N. Nikolaev for useful comments. V.R.Z. thanks the Dipartimento di Fisica dell'Università della Calabria and the Istituto Nazionale di Fisica Nucleare – gruppo collegato di Cosenza for their warm hospitality while a part of this work was done. The work was supported in part by the Ministero Italiano dell'Istruzione, dell'Università e della Ricerca and by the DFG grant # 436 RUS 17/82/06 and by the RFBR grant # 06-02-16905-a.

1. S. Adler, Phys. Rev. B **135**, 963 (1964).
2. E. A. Kuraev, L. N. Lipatov, and V. S. Fadin, Sov. Phys.

JETP **45**, 199 (1977) [ZhETF **72**, 377 (1977)]; I. I. Balitsky and L. N. Lipatov, Sov. J. Nucl. Phys. **28**, 822 (1978) [Yad. Fiz. **28**, 1597 (1978)].
3. N. N. Nikolaev, B. G. Zakharov, and V. R. Zoller, JETP Lett. **59**, 6 (1994) [Pisma v ZhETF **59**, 8 (1994)].
4. N. N. Nikolaev and B. G. Zakharov, J. Exp. Theor. Phys. **78**, 598 (1994) [ZhETF **105**, 1117 (1994)].
5. R. Fiore and V. R. Zoller, JETP Lett. **82**, 385 (2005); Phys. Lett. B **632**, 87 (2006).
6. V. Barone, M. Genovese, N. N. Nikolaev et al., Phys. Lett. B **292**, 181 (1992).
7. Y. Nambu, Phys. Rev. Lett. **4**, 380 (1960); M. Gell-Mann and M. Levy, Nuovo Cimento **17**, 705 (1960).
8. M. Diehl, T. Feldmann, R. Jakob, and R. Kroll, Eur. Phys. J. C **8**, 409 (1999).
9. A. V. Radyushkin, Phys. Rev. D **58**, 114008 (1998).
10. C. A. Piketty and L. Stodolsky, Nucl. Phys. B **15**, 571 (1970).
11. A. A. Belkov and B. Z. Kopeliovich, Sov. J. Nucl. Phys. **46**, 499 (1987).
12. B. Z. Kopeliovich, Phys. Lett. B **227**, 461 (1989); Sov. Phys. JETP **70**, 801 (1990).
13. B. Z. Kopeliovich and P. Marage, Int. J. Mod. Phys. A **8**, 1513 (1993).
14. C. Boros, J. T. Londergan, and A. W. Thomas, Phys. Rev. D **58**, 114030 (1998).
15. N. N. Nikolaev and B. G. Zakharov, Z. Phys. C **49**, 607 (1991); C **53**, 331 (1992); C **64**, 631 (1994).
16. A. H. Mueller, Nucl. Phys. B **415**, 373 (1994); A. H. Mueller and B. Patel, Nucl. Phys. B **425**, 471 (1994).
17. A. Hebecker, Phys. Rept. **331**, 1 (2000).
18. K. Golec-Biernat and M. Wüsthoff, Phys. Rev. D **59**, 014017 (1999); ibid. D **60**, 114023 (1999); H. Kowalski, L. Motyka and G. Watt, Phys. Rev. D **74**, 074016 (2006); J. R. Forshaw, G. Shaw, and R. Sandapen, JHEP **0611**, 025 (2006).
19. J. S. Bell, in *Proc. of the 11th session of the Scottish Universities Summer School in Physics*, 1970. NATO Advanced Study Institute, Eds. J. Cumming and H. Osborn, Academic Press, New York, 1971, p. 369.
20. The ACCMOR Collab., C. Daum, L. Hertzberger, W. Hoogland et al., Nucl. Phys. B **182**, 269 (1981).
21. M. L. Goldberger and S. B. Treiman, Phys. Rev. **111**, 354 (1958).
22. N. N. Nikolaev, Comments Nucl. Part. Phys. **21**, 41 (1992); N. N. Nikolaev, A. Szczurek, J. Speth et al., Nucl. Phys. A **567**, 781 (1994).
23. A. Szczurek, N. N. Nikolaev, and J. Speth, Phys. Rev. C **60**, 055206 (2002).
24. W. Jaus, Phys. Rev. D **44**, 2851 (1991).
25. N. N. Nikolaev, B. G. Zakharov, and V. R. Zoller, Phys. Lett. B **328**, 486 (1994); J. Exp. Theor. Phys. **78**, 806 (1994).
26. N. N. Nikolaev, B. G. Zakharov, and V. R. Zoller, JETP Lett. **66**, 138 (1997) [Pisma v ZhETF **66**, 134 (1997)]; N. N. Nikolaev, J. Speth, and V. R. Zoller, Phys. Lett. B **473**, 157 (2000); J. Exp. Theor. Phys. **93**, 957 (2001) [ZhETF **93**, 1104 (2001)]; Eur. Phys. J. C **22**, 637 (2002).
27. N. N. Nikolaev, W. Schäfer, B. G. Zakharov, and V. R. Zoller, Pis'ma v ZhETF **84**, 631 (2006).
28. Particle Data Group, W.-M. Yao et al., J. Phys. G **33**, 1 (2006).
29. I. P. Ivanov, N. N. Nikolaev, and W. Schäfer, Phys. Part. Nucl. **35**, 30 (2004).